

# The asymptotics of a generalised Beta function

R. B. PARIS

*Division of Computing and Mathematics,  
University of Abertay Dundee, Dundee DD1 1HG, UK*

## Abstract

We consider the generalised Beta function introduced by Chaudhry *et al.* [J. Comp. Appl. Math. **78** (1997) 19–32] defined by

$$B(x, y; p) = \int_0^1 t^{x-1} (1-t)^{y-1} \exp\left[\frac{-p}{4t(1-t)}\right] dt,$$

where  $\Re(p) > 0$  and the parameters  $x$  and  $y$  are arbitrary complex numbers. The asymptotic behaviour of  $B(x, y; p)$  is obtained when (i)  $p$  large, with  $x$  and  $y$  fixed, (ii)  $x$  and  $p$  large, (iii)  $x$ ,  $y$  and  $p$  large and (iv) either  $x$  or  $y$  large, with  $p$  finite. Numerical results are given to illustrate the accuracy of the formulas obtained.

**Mathematics Subject Classification:** 30E15, 33B15, 34E05, 41A60

**Keywords:** Generalised Beta function, asymptotic expansion, Mellin-Barnes integral, method of steepest descents

## 1. Introduction

In [1], Chaudhry *et al.* introduced a generalised beta function defined by the Euler-type integral<sup>1</sup>

$$B(x, y; p) = \int_0^1 t^{x-1} (1-t)^{y-1} \exp\left[\frac{-p}{4t(1-t)}\right] dt, \quad (1.1)$$

where  $\Re(p) > 0$  and the parameters  $x$  and  $y$  are arbitrary complex numbers. When  $p = 0$ , it is clear that when  $\Re(x) > 0$  and  $\Re(y) > 0$  the generalised function reduces to the well-known beta function  $B(x, y)$  of classical analysis. The justification for defining this extension of the beta function is given in [1] and an application of its use in defining extensions of the Gauss and confluent hypergeometric functions is discussed in [2]. It is evident from the definition in (1.1) that  $B(x, y; p)$  satisfies the symmetry property

$$B(x, y; p) = B(y, x; p). \quad (1.2)$$

A list of useful properties of  $B(x, y; p)$  is detailed by Miller in [4], where it is established that  $B(x, y; p)$  may be expanded as an infinite series of Whittaker functions or Laguerre polynomials; see (A.1). He also obtained a Mellin-Barnes integral representation for

<sup>1</sup>The factor 4 is introduced in the exponential for presentational convenience.

$B(x, y; p)$ , which we exploit in Section 2, and expressed  $B(x, x \pm n; p)$  and  $B(1 \pm n, 1; p)$ , where  $n$  is an integer, as finite sums of Whittaker functions.

Our aim in this note is to derive asymptotic expansions for  $B(x, y; p)$  for large  $x$ ,  $y$  and  $p$ . We consider (i)  $|p| \rightarrow \infty$  in  $|\arg p| < \frac{1}{2}\pi$ , with  $x$  and  $y$  fixed, (ii)  $x$  and  $p$  large, (iii)  $x$ ,  $y$  and  $p$  large and (iv) either  $x$  or  $y$  large, with  $p$  finite. The expansion for large  $p$  is obtained using a Mellin-Barnes integral representation for  $B(x, y; p)$ , whereas the other cases are obtained using the method of steepest descents.

## 2. The expansion of $B(x, y; p)$ for large $p$ with $x, y$ finite

We start with the Mellin-Barnes integral representation given by Miller [4]

$$B(x, y; p) = 2^{1-x-y} \pi^{\frac{1}{2}} \frac{1}{2\pi i} \int_{c-\infty i}^{c+\infty i} \frac{\Gamma(s)\Gamma(x+s)\Gamma(y+s)}{\Gamma(\frac{1}{2}x+\frac{1}{2}y+s)\Gamma(\frac{1}{2}x+\frac{1}{2}y+\frac{1}{2}+s)} p^{-s} ds \quad (2.1)$$

valid in  $|\arg p| < \frac{1}{2}\pi$ , where  $c > \max\{0, -\Re(x), -\Re(y)\}$  so that the integration path lies to the right of all the poles of the integrand situated at  $s = -k$ ,  $s = -x - k$  and  $s = -y - k$ ,  $k = 0, 1, 2, \dots$ . Displacement of the integration path to the left over the poles followed by evaluation of the residues (assuming that no two members of the set  $\{0, x, y\}$  differ by an integer – thereby avoiding the presence of higher-order poles) yields the result that  $B(x, y; p)$  can be expressed as the sum of three  ${}_2F_2(-\frac{1}{4}p)$  hypergeometric functions; see [4, Eq. (1.6)].

Since there are no poles in the half-plane  $\Re(s) > c$  it follows that displacement of the integration path to the right can produce no algebraic-type asymptotic expansion; see [8, §5.4]. We can therefore displace the path as far to the right as we please; on such a displaced path, which we denote by  $L$ , the variable  $|s|$  is everywhere large. The ratio of gamma functions in the integrand in (2.1) may then be expanded as an inverse factorial expansion given by [8, p. 39, Lemma 2.2]

$$\frac{\Gamma(s)\Gamma(x+s)\Gamma(y+s)}{\Gamma(\frac{1}{2}x+\frac{1}{2}y+s)\Gamma(\frac{1}{2}x+\frac{1}{2}y+\frac{1}{2}+s)} = \sum_{j=0}^{M-1} (-)^j c_j \Gamma(s-j-\frac{1}{2}) + \rho_M(s) \Gamma(s-M-\frac{1}{2}),$$

where  $M$  is a positive integer and  $\rho_M(s) = O(1)$  as  $|s| \rightarrow \infty$  in  $|\arg s| < \pi$ . The coefficients  $c_j \equiv c_j(x, y)$  are discussed below where the leading coefficient  $c_0 = 1$ .

Substitution of the above inverse factorial expansion into the integral (2.1) then produces

$$B(x, y; p) = 2^{1-x-y} \pi^{\frac{1}{2}} \left\{ \sum_{j=0}^{M-1} (-)^j c_j \frac{1}{2\pi i} \int_L \Gamma(s-j-\frac{1}{2}) p^{-s} ds + R_M \right\},$$

where

$$R_M = \frac{1}{2\pi i} \int_L \rho_M(s) \Gamma(s-M-\frac{1}{2}) p^{-s} ds.$$

The integral may be evaluated by the well-known Cahen-Mellin integral given by (see, for example, [8, p. 90])

$$\frac{1}{2\pi i} \int_{c-\infty i}^{c+\infty i} \Gamma(s+\alpha) z^{-s} ds = z^\alpha e^{-z} \quad (|\arg z| < \frac{1}{2}\pi, \quad c > -\Re(\alpha))$$

to yield

$$B(x, y; p) = 2^{1-x-y} \pi^{\frac{1}{2}} \left\{ p^{-\frac{1}{2}} e^{-p} \sum_{j=0}^{M-1} (-)^j c_j p^{-j} + R_M \right\}.$$

A bound for the remainder  $R_M$  has been considered in [8, p. 71, Lemma 2.7], from which it follows that  $R_M = O(p^{-M-\frac{1}{2}} e^{-p})$  as  $|p| \rightarrow \infty$  in  $|\arg p| < \frac{1}{2}\pi$ .

Hence we obtain the asymptotic expansion

$$B(x, y; p) = 2^{1-x-y} \pi^{\frac{1}{2}} p^{-\frac{1}{2}} e^{-p} \left\{ \sum_{j=0}^{M-1} (-)^j c_j p^{-j} + O(p^{-M}) \right\} \quad (2.2)$$

valid as  $|p| \rightarrow \infty$  in the sector  $|\arg p| < \frac{1}{2}\pi$ . The expansion of  $B(x, y; p)$  for large  $p$  is seen to be exponentially small in  $|\arg p| < \frac{1}{2}\pi$ ; this is a standard result when there are no poles on the right of the path in (2.1) and routine path displacement does not produce any useful asymptotic information [8, §5.4].

The coefficients  $c_j$  for  $j \geq 1$  can be generated by the algorithm described in [8, §2.2.4]. It is found that

$$\begin{aligned} c_1 &= \frac{1}{4}(1 + x + y + 2xy - x^2 - y^2), \\ c_2 &= \frac{1}{32}(9 + 6(2 + xy)(x + y + xy) - (7 + 4xy)(x^2 + y^2) - 6(x^3 + y^3) + x^4 + y^4 + 14xy), \end{aligned}$$

which are symmetrical in  $x$  and  $y$  as required by (1.2). A closed-form representation for  $c_j$  is derived in the appendix, where it is shown that  $c_j$  can be expressed in terms of a terminating  ${}_3F_2(1)$  hypergeometric function given by

$$c_j \equiv c_j(x, y) = \frac{(\frac{1}{2})_j (y + \frac{1}{2})_j}{j!} {}_3F_2 \left[ \begin{matrix} -j, \frac{1}{2}y - \frac{1}{2}x, \frac{1}{2}y - \frac{1}{2}x + \frac{1}{2} \\ \frac{1}{2}, y + \frac{1}{2} \end{matrix}; 1 \right], \quad (2.3)$$

where  $(a)_j = \Gamma(a+j)/\Gamma(a)$  is the Pochhammer symbol. When  $x = y$ , this reduces to the simpler expression

$$c_j(x, x) = \frac{(\frac{1}{2})_j (x + \frac{1}{2})_j}{j!}. \quad (2.4)$$

We remark that the asymptotic expansion of  $B(x, y; p)$  for  $p \rightarrow \infty$  could also have been obtained by application of the method of steepest descents, which we shall employ in the subsequent sections. See also the appendix for a different approach.

### 3. The expansion of $B(x, y; p)$ for large $x$ and $p$ with $y$ finite

We consider the expansion of  $B(x, y; p)$  for large  $x$  and  $p$ , with  $y$  finite, when it is supposed that  $p = ax$ , where  $a > 0$  and  $|\arg x| < \frac{1}{2}\pi$ . By the symmetry property (1.2), the same result will also cover the case of large  $y$  and  $p$ , with  $x$  finite. From (1.1), we have

$$B(x, y; ax) = \int_0^1 f(t) e^{-x\psi(t)} dt \quad (|\arg x| < \frac{1}{2}\pi), \quad (3.1)$$

where

$$\psi(t) = \frac{a}{4t(1-t)} - \log t, \quad f(t) = \frac{(1-t)^y}{t}.$$

Saddle points of the exponential factor are given by  $\psi'(t) = 0$ ; that is, at the roots of the cubic

$$t(1-t)^2 + \frac{1}{4}a(1-2t) = 0. \quad (3.2)$$

We label the three saddles  $t_0$ ,  $t_1$  and  $t_2$ . All three saddles lie on the real axis with  $t_0$  situated in the closed interval  $[0, 1]$ , with  $t_1 > 1$  and  $t_2 < 0$ . The  $t$ -plane is cut along  $(-\infty, 0]$ . Paths of steepest descent through the saddles  $t_r$  ( $r = 0, 1$ ) are given by

$$\Im\{e^{i\theta}(\psi(t) - \psi(t_r))\} = 0, \quad \theta = \arg x;$$

these paths terminate at  $t = 0$  and  $t = 1$  in the directions  $|\theta - \phi| < \frac{1}{2}\pi$  and  $\frac{1}{2}\pi < \theta - \phi < \frac{3}{2}\pi$ , respectively, where  $\phi = \arg t$ .

When  $x > 0$ , the integration path coincides with the steepest descent path over the saddle  $t_0$ ; for complex  $x$  in the sector  $|\arg x| < \frac{1}{2}\pi$ , the steepest descent path through  $t_0$  becomes deformed but still terminates at  $t = 0$  and  $t = 1$ ; see Fig. 1. Application of the

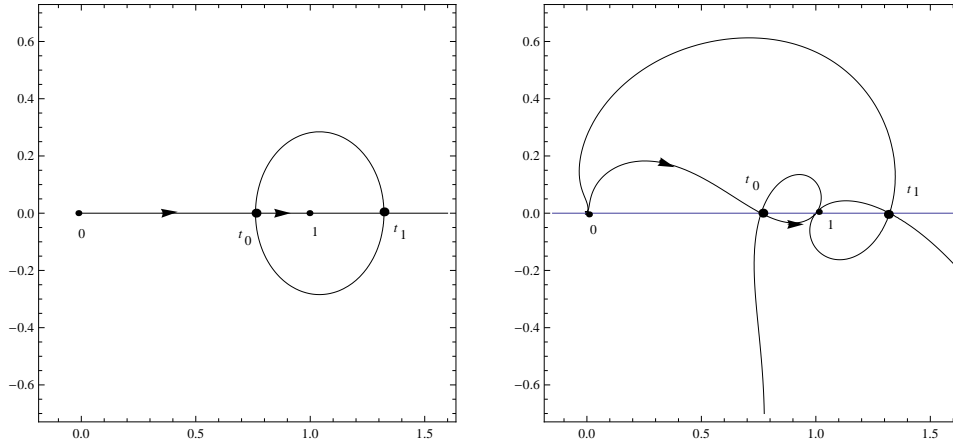


Figure 1: The steepest descent and ascent paths through the saddles  $t_0$  and  $t_1$  (heavy dots) when  $a = 1/3$  and (a)  $\theta = 0$  and (b)  $\theta = \pi/4$ . The arrows indicate the integration path. In (b) the steepest ascent paths spiral round  $t = 0$  out to infinity passing onto adjacent Riemann surfaces. The saddle  $t_2$  on the branch cut on  $(-\infty, 0]$  is not shown.

saddle-point method then yields the leading behaviour

$$\begin{aligned} B(x, y; ax) &\sim \sqrt{\frac{2\pi}{x\psi''(t_0)}} f(t_0) e^{-x\psi(t_0)} \\ &= \sqrt{\frac{2\pi}{x\psi''(t_0)}} t_0^{x-1} (1-t_0)^{y-1} \exp\left[\frac{-ax}{4t_0(1-t_0)}\right] \end{aligned} \quad (3.3)$$

as  $|x| \rightarrow \infty$  in the sector  $|\arg x| < \frac{1}{2}\pi$ , where some routine algebra combined with (3.2) shows that

$$\psi''(t_0) = \frac{1 - 3t_0 + 4t_0^2}{t_0^2(1-t_0)(2t_0-1)}.$$

We remark that the saddle  $t_0 \equiv t_0(a)$  has to be computed for a particular value of the parameter  $a$ , either directly from (3.2) or as a cubic root.

The asymptotic expansion of  $B(x, y; ax)$  is given by [7, p. 47]

$$B(x, y; ax) \sim 2e^{-x\psi(t_0)} \sum_{n=0}^{\infty} \frac{C_{2n}\Gamma(n+\frac{1}{2})}{x^{n+\frac{1}{2}}} \quad (|x| \rightarrow \infty, |\arg x| < \frac{1}{2}\pi). \quad (3.4)$$

The coefficients  $C_n$  can be obtained by an inversion process and are listed for  $n \leq 8$  in [3, p. 119] and for  $n \leq 4$  in [9, p. 13]. Alternatively, they can be obtained by an expansion process to yield Wojdyło's formula [10] given by

$$C_n = \frac{1}{2a_0^{(n+1)/2}} \sum_{k=0}^n b_{n-k} \sum_{j=0}^k \frac{(-)^j (\frac{1}{2}n + \frac{1}{2})_j}{j! a_0^j} B_{kj}; \quad (3.5)$$

see also [5, 6]. Here  $B_{kj} \equiv B_{kj}(a_1, a_2, \dots, a_{k-j+1})$  are the partial ordinary Bell polynomials generated by the recursion<sup>2</sup>

$$B_{kj} = \sum_{r=1}^{k-j+1} a_r B_{k-r, j-1}, \quad B_{k0} = \delta_{k0},$$

where  $\delta_{mn}$  is the Kronecker symbol, and the coefficients  $a_r$  and  $b_r$  appear in the expansions

$$\psi(t) - \psi(t_0) = \sum_{r=0}^{\infty} a_r (t - t_0)^{r+2}, \quad f(t) = \sum_{r=0}^{\infty} b_r (t - t_0)^r \quad (3.6)$$

valid in a neighbourhood of the saddle  $t = t_0$ .

In numerical computations we choose a value of the parameter  $a$  and compute the saddle  $t_0$  from (3.2). With a value of  $y$ , *Mathematica* is used to determine the coefficients  $a_r$  and  $b_r$  for  $0 \leq r \leq n_0$ . The coefficients  $C_{2n}$  can then be calculated for  $0 \leq n \leq n_0$  from (3.5). We display the computed values of  $C_{2n}$  for different values of  $a$  and  $y$  in Table 1. In Table 2, the values of the absolute relative error in the computation of  $B(x, y; ax)$  from (3.4) are presented as a function of the truncation index  $n$  when  $x = 100$ .

Table 1: Values of the coefficients  $C_{2n}$  (to 10dp) for different  $a$  and  $y$ .

$n$	$a = 1, y = 1$	$a = \frac{1}{2}, y = \frac{3}{2}$	$a = \frac{3}{2}, y = \frac{5}{4}$	$a = 2, y = \frac{1}{2}$
0	+0.2668661228	+0.1364219142	+0.2036093538	+0.3909054941
1	+0.0982652355	+0.2683838462	+0.0762869817	-0.0309094064
2	-0.0635656655	-0.1085963949	-0.0456489054	-0.0039290992
3	+0.0186002666	+0.0151339630	+0.0137423943	+0.0024209801
4	-0.0039253710	-0.0003383888	-0.0026770977	-0.0005115807
5	+0.0012059654	+0.0004533741	+0.0003423270	+0.0000299402

#### 4. The expansion of $B(x, y; p)$ for large $x, y$ and $p$

We consider the expansion of  $B(x, y; p)$  for large  $x, y$  and  $p$ , when it is supposed that  $p = ax$  and  $y = bx$ , where  $a > 0, b > 0$  and  $|\arg x| < \frac{1}{2}\pi$ . From (1.1), we have

$$B(x, y; p) = \int_0^1 f(t) e^{-x\psi(t)} dt \quad (|\arg x| < \frac{1}{2}\pi), \quad (4.1)$$

<sup>2</sup>For example, this generates the values  $B_{41} = a_4$ ,  $B_{42} = a_3^2 + 2a_1a_3$ ,  $B_{43} = 3a_1^2a_2$  and  $B_{44} = a_1^4$ .

Table 2: Values of the absolute relative error in  $B(x, y; ax)$  when  $x = 100$  for different truncation index.

$n$	$a = 1, y = 1$	$a = \frac{1}{2}, y = \frac{3}{2}$	$a = \frac{3}{2}, y = \frac{5}{4}$	$a = 2, y = \frac{1}{2}$
0	$1.838 \times 10^{-3}$	$9.682 \times 10^{-3}$	$1.853 \times 10^{-3}$	$3.963 \times 10^{-4}$
1	$1.770 \times 10^{-5}$	$5.892 \times 10^{-5}$	$1.666 \times 10^{-5}$	$7.426 \times 10^{-7}$
2	$1.295 \times 10^{-7}$	$2.058 \times 10^{-7}$	$1.255 \times 10^{-7}$	$1.153 \times 10^{-8}$
3	$9.506 \times 10^{-10}$	$1.517 \times 10^{-10}$	$8.562 \times 10^{-10}$	$8.568 \times 10^{-11}$
4	$1.295 \times 10^{-11}$	$9.526 \times 10^{-12}$	$5.011 \times 10^{-12}$	$2.332 \times 10^{-13}$
5	$3.688 \times 10^{-12}$	$1.933 \times 10^{-13}$	$5.472 \times 10^{-14}$	$6.917 \times 10^{-15}$

where

$$\psi(t) = \frac{a}{4t(1-t)} - \log t - b \log(1-t), \quad f(t) = \frac{1}{t(1-t)}. \quad (4.2)$$

Saddle points of the exponential factor are given by the roots of the cubic

$$t(1-t)\{1 - (b+1)t\} + \frac{1}{4}a(1-2t) = 0. \quad (4.3)$$

Routine examination of this cubic shows that, when  $a > 0$ ,  $b > 0$ , all roots are real, with one root greater than 1, one in the interval  $[0, 1]$  and one negative root. The distribution of the saddles is thus similar to that in Section 3, where we continue to label the saddle situated in  $[0, 1]$  by  $t_0$ . The topology of the path of steepest descent through the saddle  $t_0$ , given by  $\Im\{e^{i\theta}(\psi(t) - \psi(t_0))\} = 0$  where  $\theta = \arg x$ , is also similar to that depicted in Fig. 1.

Accordingly, the expansion of  $B(x, y; p)$  when  $p = ax$  and  $y = bx$ , with  $a > 0$ ,  $b > 0$ , is given by

$$B(x, bx; ax) \sim 2e^{-x\psi(t_0)} \sum_{n=0}^{\infty} \frac{C_{2n}\Gamma(n + \frac{1}{2})}{x^{n+\frac{1}{2}}} \quad (|x| \rightarrow \infty, |\arg x| < \frac{1}{2}\pi), \quad (4.4)$$

where the coefficients  $C_{2n}$  can be determined from (3.5) when the coefficients  $a_r$  and  $b_r$  in (3.6) are evaluated from the definitions of  $\psi(t)$  and  $f(t)$  in (4.2).

The leading behaviour is

$$\begin{aligned} B(x, bx; ax) &\sim \sqrt{\frac{2\pi}{x\psi''(t_0)}} f(t_0) e^{-x\psi(t_0)} \\ &= \sqrt{\frac{2\pi}{x\psi''(t_0)}} t_0^{x-1} (1-t_0)^{bx-1} \exp\left[\frac{-ax}{4t_0(1-t_0)}\right] \end{aligned} \quad (4.5)$$

as  $|x| \rightarrow \infty$  in the sector  $|\arg x| < \frac{1}{2}\pi$ , where

$$\psi''(t_0) = \frac{1 - 3t_0 + 4t_0^2}{t_0^2(1-t_0)(2t_0-1)} \left(1 - \frac{bt_0}{1-t_0}\right) + \frac{b}{t_0(1-t_0)^2}$$

and  $t_0 \equiv t_0(a, b)$  is the root of (4.3) situated in  $t \in [0, 1]$ .

We note that when  $b = 1$  we have the result [1, 4]

$$B(x, x; p) = 2^{1-2x} \pi^{\frac{1}{2}} p^{(x-1)/2} e^{-\frac{1}{2}p} W_{-\frac{1}{2}x, \frac{1}{2}x}(p)$$

in terms of the Whittaker function  $W_{\kappa, \mu}(z)$ ; see (A.1).

### 5. The behaviour of $B(x, y; p)$ for large $x$ and finite $y$ and $p$

In this final section, we examine the behaviour of  $B(x, y; p)$  for large complex  $x = |x|e^{i\theta}$ , with  $0 \leq \theta \leq \pi$ , when  $y$  and  $p > 0$  are finite. The situation when  $-\pi \leq \theta \leq 0$  is analogous and, in the case of real  $y$ ,  $B(x, y; p)$  assumes conjugate values. This case has been discussed in [2, Appendix], but is repeated (with minor corrections) here for completeness. By the symmetry property (1.2), the same result will also cover the case of large  $y$ , with  $x$  and  $p$  finite.

From (1.1), we have upon interchanging  $x$  and  $y$  (by virtue of (1.2))

$$B(x, y; p) = \int_0^1 f(t) e^{-|x|\psi(t)} dt, \quad (5.1)$$

where

$$\psi(t) = \frac{\alpha}{t(1-t)} - e^{i\theta} \log(1-t), \quad f(t) = \frac{t^{y-1}}{1-t}, \quad \alpha := \frac{p}{4|x|}. \quad (5.2)$$

Because  $p > 0$  is a fixed parameter, the integral (5.1) is valid for arbitrary complex values of  $x$  and  $y$ . Saddle points of the exponential factor arise when  $\psi'(t) = 0$ ; that is, when

$$t^2(t-1) + \alpha e^{-i\theta}(1-2t) = 0. \quad (5.3)$$

We label the three saddles  $t_0$ ,  $t_1$  and  $t_2$  as in Section 3. When  $\theta = 0$ , all three saddles are situated on the real axis with  $t_0 \in [0, 1]$  and  $t_1 > 1$ ,  $t_2 < 1$ . As  $\theta$  increases, the saddles  $t_0$  and  $t_2$  rotate about the origin and  $t_1$  rotates about the point  $t = 1$ . The result of this rotation is that, when  $\theta = \pi$ ,  $t_0$  and  $t_2$  become a complex conjugate pair near the origin and  $t_1$  is situated in the interval  $[0, 1]$ ; see Fig. 2.

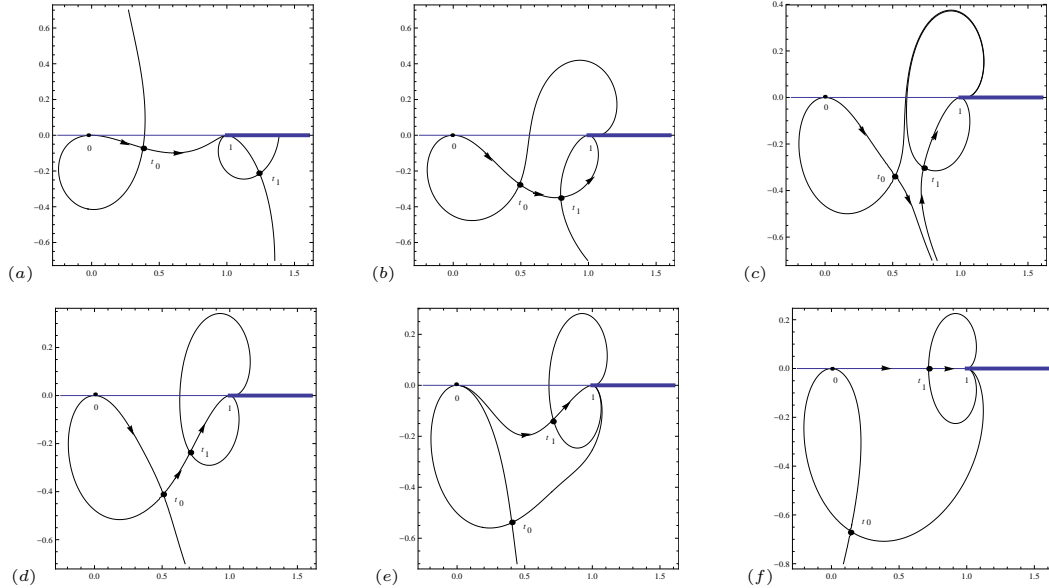


Figure 2: The steepest descent and ascent paths through the saddles  $t_0$  and  $t_1$  (heavy dots) when  $\alpha = 1/3$  and (a)  $\theta = 0.25\pi$ , (b)  $\theta = \theta_0 = 0.65595\pi$ , (c)  $\theta = 0.69\pi$ , (d)  $\theta = \theta_1 = 0.71782\pi$ , (e)  $\theta = 0.80\pi$  and (f)  $\theta = \pi$ . The arrows indicate the integration path. The steepest ascent paths spiral round  $t = 1$  out to infinity passing onto adjacent Riemann surfaces. The saddle  $t_2$  is not shown. The  $t$ -plane is cut along  $[1, \infty)$ .

When  $\theta = 0$ , the integration path coincides with the steepest descent path passing over the saddle  $t_0$  given approximately by

$$t_0 \simeq \alpha^{\frac{1}{2}} - \frac{1}{2}\alpha \quad (x \rightarrow \infty).$$

Then, with the estimates

$$x\psi(t_0) \simeq (px)^{1/2} + \frac{3}{8}p, \quad \psi''(t_0) \simeq 2\alpha^{-\frac{1}{2}},$$

we find by application of the saddle-point method the leading behaviour

$$B(x, y; p) \sim \sqrt{\frac{\pi}{x}} \left(\frac{p}{4x}\right)^{\frac{1}{2}y - \frac{1}{4}} \exp\left[-(px)^{1/2} - \frac{3}{8}p\right] \quad (\theta = 0, x \rightarrow +\infty). \quad (5.4)$$

When  $\theta = \pi$ , we find from (5.3) that the saddle  $t_1$  close to the point  $t = 1$  is given by

$$t_1 \simeq 1 - \alpha + \alpha^3 \quad (|x| \rightarrow \infty)$$

and

$$|x|\psi(t_1) \simeq |x| + \frac{1}{4}p - |x|\log \alpha, \quad \psi''(t_1) \simeq \alpha^{-2}.$$

The integration path again coincides with the steepest descent path through  $t_1$ , and so we obtain the behaviour

$$\begin{aligned} B(x, y; p) &\sim i\sqrt{\frac{2\pi}{x}} \left(\frac{p}{4x}\right)^x e^{\pi i x} \exp\left[x - \frac{1}{4}p\right] \quad (\theta = \pi, x \rightarrow -\infty) \\ &= \sqrt{\frac{2\pi}{|x|}} \left(\frac{p}{4|x|}\right)^{-|x|} \exp\left[-|x| - \frac{1}{4}p\right]. \end{aligned} \quad (5.5)$$

The leading terms in (5.4) and (5.5) were given in [2, Appendix].

A detailed study of the topology of the steepest descent paths<sup>3</sup> through the saddles  $t_0$  and  $t_1$  when  $0 \leq \theta \leq \pi$  is summarised in Fig. 2 for the particular case  $\alpha = \frac{1}{3}$ . The  $t$ -plane is cut along  $[1, \infty)$  and paths of steepest descent either terminate at  $t = 0$  (with  $|\arg t| < \frac{1}{2}\pi$ ),  $t = 1$  (with  $|\arg(1 - t)| < \frac{1}{2}\pi$ ) or at infinity. Paths that approach infinity spiral round the point  $t = 1$  passing onto adjacent Riemann surfaces. The figures reveal that there are two critical values of the phase  $\theta$ , where the saddles  $t_0$  and  $t_1$  become connected (via a Stokes phenomenon). We denote these values by  $\theta_0 \equiv \theta_0(\alpha)$  and  $\theta_1 \equiv \theta_1(\alpha)$ , where  $\alpha$  is defined in (5.2). The values of these critical angles are tabulated in Table 3 for different  $\alpha$ .

When  $0 \leq \theta < \theta_0(\alpha)$ , the integration path can be deformed to coincide with the steepest descent path passing over  $t_0$ , so that the leading behaviour in (5.4) applies in this sector. When  $\theta_0(\alpha) < \theta < \theta_1(\alpha)$ , the integration path is deformed to pass over both saddles  $t_0$  and  $t_1$ , where each steepest descent path spirals out to infinity. Finally, when  $\theta_1(\alpha) < \theta \leq \pi$ , the integration path is deformed to pass over only the saddle  $t_1$ .

Based on these considerations and on the approximation of the saddles  $t_0 \simeq \alpha'^{\frac{1}{2}} - \frac{1}{2}\alpha'$ ,  $t_1 \simeq 1 + \alpha' - \alpha'^3$ , where  $\alpha' = p/(4x)$ , the leading behaviour of  $B(x, y; p)$  is found to be

$$B(x, y; p) \sim \begin{cases} J_0 & 0 \leq \theta < \theta_1(\alpha) \\ J_0 - J_1 & \theta_1(\alpha) < \theta < \theta_2(\alpha) \\ J_1 & \theta_2(\alpha) < \theta \leq \pi \end{cases} \quad (5.6)$$

---

<sup>3</sup>The saddle  $t_2$  does not enter into our consideration as it plays no role in the asymptotic evaluation of  $B(x, y; p)$  when  $0 \leq \theta \leq \pi$ .



Table 3: Values of the critical angles  $\theta_0$ ,  $\theta_1$  and  $\theta^*$  as a function of  $\alpha = p/(4|x|)$ .

$\alpha$	$\theta_0/\pi$	$\theta_1/\pi$	$\theta^*/\pi$
0.30	0.603324	0.752315	0.688289
0.25	0.536784	0.798621	0.681218
0.20	0.476795	0.840611	0.672858
0.15	0.418651	0.879708	0.662628
0.10	0.358268	0.916935	0.649359
0.05	0.288029	0.953688	0.629820
0.01	0.198480	0.986248	0.597144

as  $|x| \rightarrow \infty$  when  $0 \leq \theta \leq \pi$  (with  $y$  and  $p > 0$  finite), where

$$\begin{aligned}
J_0 &:= \sqrt{\frac{2\pi}{|x|\psi''(t_0)}} t_0^{y-1} (1-t_0)^{x-1} \exp\left[\frac{-p}{4t_0(1-t_0)}\right] \\
&\sim \sqrt{\frac{\pi}{x}} \left(\frac{p}{4x}\right)^{\frac{1}{2}y-\frac{1}{4}} \exp\left[-(px)^{1/2} - \frac{3}{8}p\right]
\end{aligned} \tag{5.7}$$

and

$$\begin{aligned}
J_1 &:= \sqrt{\frac{2\pi}{|x|\psi''(t_1)}} t_1^{y-1} (1-t_1)^{x-1} \exp\left[\frac{-p}{4t_1(1-t_1)}\right] \\
&\sim i\sqrt{\frac{2\pi}{x}} \left(\frac{p}{4x}\right)^x e^{\pi ix} \exp\left[x - \frac{1}{4}p\right]
\end{aligned} \tag{5.8}$$

with  $\arg \psi''(t_r) \in [0, 2\pi]$ ,  $r = 0, 1$ . Inspection of Table 3 shows that as  $\alpha$  decreases (that is, as  $|x|$  increases for fixed  $p$ ) the angular sector  $\theta_0(\alpha) \leq \theta \leq \theta_1(\alpha)$ , where  $B(x, y; p)$  receives a contribution from both saddles, increases. We also show in Table 3 the value of  $\theta = \theta^*(\alpha)$  at which  $\Re(\psi(t_0)) = \Re(\psi(t_1))$  when the saddles are of the same height. We have  $\theta_0(\alpha) < \theta^*(\alpha) < \theta_1(\alpha)$ ; then, for  $\theta < \theta^*(\alpha)$  the saddle  $t_0$  is dominant, whereas when  $\theta > \theta^*(\alpha)$  the saddle  $t_1$  is dominant in the large- $|x|$  limit.

In Table 4 we present the results of numerical calculations using the asymptotic behaviour of  $B(x, y; p)$  in (5.6) compared to the values obtained by numerical integration of (5.1). The parameter values chosen correspond to  $\alpha = 0.01$  and the saddles  $t_0$  and  $t_1$  are computed from (5.3), with the leading forms  $J_0$  and  $J_1$  computed from (5.7) and (5.8). It is seen from Table 3 that the exchange of dominance between the two contributory saddles arises for  $\theta \simeq 0.60\pi$ .

### Appendix: A closed-form expression for the coefficients $c_j$

In this appendix we derive a closed-form expression for the coefficients  $c_j$  appearing in the expansion (2.2). Miller [4, Eq. (2.3a)] has shown that  $B(x, y; p)$  can be expressed as a convergent series of Whittaker functions in the form

$$B(x, y; p) = 2^{1-x-y} \pi^{\frac{1}{2}} p^{(y-1)/2} e^{-\frac{1}{2}p} \sum_{k=0}^{\infty} \frac{(\frac{1}{2}y - \frac{1}{2}x)_k (\frac{1}{2} + \frac{1}{2}y - \frac{1}{2}x)_k}{k!} W_{-k-\frac{1}{2}y, \frac{1}{2}y}(p), \tag{A.1}$$

Table 4: Values of the asymptotic behaviour of  $B(x, y; p)$  in (5.6) with the calculated value when  $|x| = 50$ ,  $p = 2$  ( $\alpha = 0.01$ ) and  $y = \frac{1}{2}$  for different  $\theta = \arg x$ .

$\theta/\pi$	Asymptotic value	Calculated value
0	$+5.175 \times 10^{-06}$	$+5.187 \times 10^{-06}$
0.20	$-8.210 \times 10^{-06} + 2.081 \times 10^{-06}i$	$-8.223 \times 10^{-06} + 2.096 \times 10^{-06}i$
0.40	$+3.468 \times 10^{-05} - 6.934 \times 10^{-06}i$	$+3.470 \times 10^{-05} - 7.020 \times 10^{-06}i$
0.50	$+2.647 \times 10^{-06} - 9.853 \times 10^{-05}i$	$+2.402 \times 10^{-06} - 9.855 \times 10^{-05}i$
0.60	$-8.837 \times 10^{-04} - 3.821 \times 10^{-03}i$	$-8.781 \times 10^{-04} - 3.823 \times 10^{-03}i$
0.70	$-5.944 \times 10^{+28} + 1.659 \times 10^{+28}i$	$-5.952 \times 10^{+28} + 1.652 \times 10^{+28}i$
0.80	$+2.786 \times 10^{+54} + 3.451 \times 10^{+54}i$	$+2.786 \times 10^{+54} + 3.459 \times 10^{+54}i$
1.00	$+4.146 \times 10^{+77}$	$+4.154 \times 10^{+77}$

where  $W_{\kappa, \mu}(x)$  is the Whittaker function. For  $p \rightarrow \infty$  with bounded  $k$ , we have the expansion [7, Eq. (13.19.3)]

$$W_{-k-\frac{1}{2}y, \frac{1}{2}y}(p) = p^{-k-\frac{1}{2}} e^{-\frac{1}{2}p} \left\{ \sum_{n=0}^{N-1} (-)^n \frac{(\frac{1}{2}+k)_n (y+\frac{1}{2}+k)_n}{n! p^n} + O(p^{-N}) \right\},$$

where  $N$  is a positive integer. Then we obtain from (A.1)

$$B(x, y; p) = 2^{1-x-y} \pi^{\frac{1}{2}} p^{-\frac{1}{2}} e^{-p} \{S(x, y; p) + O(p^{-N})\}, \quad (\text{A.2})$$

where

$$\begin{aligned} S(x, y; p) &= \sum_{k=0}^{N-1} \frac{(\frac{1}{2}y-\frac{1}{2}x)_k (\frac{1}{2}+\frac{1}{2}y-\frac{1}{2}x)_k}{k! p^k} \sum_{n=0}^{N-1} (-)^n \frac{(\frac{1}{2}+k)_n (y+\frac{1}{2}+k)_n}{n! p^n} \\ &= \sum_{k=0}^{N-1} \frac{(\frac{1}{2}y-\frac{1}{2}x)_k (\frac{1}{2}+\frac{1}{2}y-\frac{1}{2}x)_k}{k!} \sum_{j=k}^{N-1} (-)^{j-k} \frac{(\frac{1}{2}+k)_{j-k} (y+\frac{1}{2}+k)_{j-k}}{(j-k)! p^j} + O(p^{-N}) \end{aligned}$$

and we have made the change of summation index  $n \rightarrow j - k$ . Use of the fact that  $(-j)_k = (-)^k j! / (j - k)!$ , the above double sum can be written as

$$\begin{aligned} &\sum_{k=0}^{N-1} \frac{(\frac{1}{2}y-\frac{1}{2}x)_k (\frac{1}{2}+\frac{1}{2}y-\frac{1}{2}x)_k}{k!} \sum_{j=k}^{N-1} \frac{(-)^j}{j!} \frac{\Gamma(j+\frac{1}{2})\Gamma(y+j+\frac{1}{2})}{\Gamma(k+\frac{1}{2})\Gamma(y+\frac{1}{2}+k)p^j} \\ &= \sum_{j=0}^{N-1} \frac{(-)^j}{j!} \frac{(\frac{1}{2})_j (y+\frac{1}{2})_j}{j! p^j} \sum_{k=0}^j \frac{(-j)_k (\frac{1}{2}y-\frac{1}{2}x)_k (\frac{1}{2}+\frac{1}{2}y-\frac{1}{2}x)_k}{k! (\frac{1}{2})_k (y+\frac{1}{2})_k} \\ &= \sum_{j=0}^{N-1} \frac{(-)^j}{j!} \frac{(\frac{1}{2})_j (y+\frac{1}{2})_j}{j! p^j} {}_3F_2 \left[ \begin{matrix} -j, \frac{1}{2}y-\frac{1}{2}x, \frac{1}{2}+\frac{1}{2}y-\frac{1}{2}x \\ \frac{1}{2}, y+\frac{1}{2} \end{matrix} ; 1 \right]. \end{aligned} \quad (\text{A.3})$$

upon reversal of the order of summation and identification of the inner sum over  $k$  as a terminating  ${}_3F_2$  series of unit argument.

Comparison of (A.2) and (A.3) with the expansion obtained in (2.2) then yields the final result

$$c_j = \frac{(\frac{1}{2})_j (y+\frac{1}{2})_j}{j!} {}_3F_2 \left[ \begin{matrix} -j, \frac{1}{2}y-\frac{1}{2}x, \frac{1}{2}+\frac{1}{2}y-\frac{1}{2}x \\ \frac{1}{2}, y+\frac{1}{2} \end{matrix} ; 1 \right]. \quad (\text{A.4})$$

## References

- [1] M. A. Chaudhry, A. Qadir, M. Rafique and S. M. Zubair, Extension of Euler's beta function, *J. Comp. Appl. Math.* **78** (1997) 19–32.
- [2] M. A. Chaudhry, A. Qadir, H. M. Srivastava and R. B. Paris, Extended hypergeometric and confluent hypergeometric functions, *Appl. Math. Comp.* **159** (2004) 589–602.
- [3] R. B. Dingle, *Asymptotic Expansions: Their Derivation and Interpretation*, Academic Press, London, 1973.
- [4] A. R. Miller, Remarks on a generalized beta function, *J. Comp. Appl. Math.* **100** (1998) 23–32.
- [5] J. L. López and P. J. Pagola, An explicit formula for the coefficients of the saddle point method, *Constr. Approx.* **33** (2011) 145–162.
- [6] G. Nemes, An explicit formula for the coefficients in Laplace's method by Lagrange interpolation, *Constr. Approx.* **38** (2013) 471–487.
- [7] F. W. J. Olver, D. W. Lozier, R. F. Boisvert and C. W. Clark (eds.), *NIST Handbook of Mathematical Functions*, Cambridge University Press, Cambridge, 2010.
- [8] R. B. Paris and D. Kaminski, *Asymptotics and Mellin-Barnes Integrals*, Cambridge University Press, Cambridge, 2001.
- [9] R. B. Paris, *Hadamard Expansions and Hyperasymptotic Evaluation: An Extension of the Method of Steepest Descents*, Cambridge University Press, Cambridge, 2011.
- [10] J. Wojdyło, On the coefficients that arise from Laplace's method, *J. Comp. Appl. Math.* **196** (2006) 241–266.